

# GEOLOGICAL MAPPING USING FRACTAL TECHNIQUE

K.M. Lawal, M.N. Umego and S.B. Ojo

Department of Physics, Ahmadu Bello University, Zaria.

Email:kola2lawal@yahoo.com

(Submitted: 20 October, 2006. Accepted: 18 August, 2006)

## Abstract

*In this work the use of fractal scaling exponents for geological mapping was first investigated using theoretical models, and results from the analysis showed that the scaling exponents mapped isolated bodies but did not properly resolve bodies close to each other. However application on real data (the Mamfe basin, the Gongola basin and the Younger granite province in Nigeria) showed good correlation with the geological maps of the areas. The results also indicated that basement rocks can generally be represented by scaling exponents with values ranging between -3.0 and -2.0.*

**Keywords:** Fractal, dimension, susceptibility, spectra, scaling exponent

## 1.0 Introduction

In the past few decades, it has been a general idea in geophysics that field data arise from the interaction of some physical field (electric, magnetic, gravity, seismic and so on) with a distinct geometrical structure which consists of some geometrical units (layers, dikes, domes, faults) with smooth interfaces and homogeneous physical properties (conductivities, velocities, and so on). Geophysicists of course know quite well that nature is much more complicated: the interfaces are not smooth and the rocks are not homogeneous. Until recent years, no appropriate mathematical tools existed to analyze the heterogeneity of real objects. Today the theory of fractals allows qualitative description of the heterogeneity of real geological formations. Fractals are usually analyzed using spectral techniques because the scaling law, such as the power law dependence are preserved by Fourier transforms (Voss, 1988). The spectral slope (known as scaling exponent) is a measure of the scaling behavior of the distribution. Pilkington and Todoeschuck (1993) derived scaling exponents from susceptibility logs of Ontario and found a sufficient difference between the values for sedimentary and igneous sections. In their work it was discovered that the scaling exponent ranges from -1.96 to -1.32 for sedimentary and from -2.72 to -2.08 for igneous rocks. Maus and Dimri (1995) investigated whether this difference can also be observed from aeromagnetic data over an area of known geology. By using a small window, a profile was taken across their area of study and it was

discovered that the derived scaling exponent turns out to be a continuous function of the position of the window. Three different geological sections along the profile were clearly reflected in the values of the scaling exponent. In this work, the correlation of the scaling exponent with local geology was first investigated by using theoretical data and the results were later applied to real data.

## 2.0 Theory of Fractals

A fractal is any entity that is scale invariant. This means that it looks similar at a greater variety of scales, that is, they are self-similar. Scale invariance of a geological phenomena is of great importance in geology. It is often pointed out that an object that defines the scale, that is, a coin, a rock hammer or a person, must be included whenever a photograph of a geological feature is taken. Without the scale it is impossible to determine whether the photograph covers 10 cm or 10 km. Also without an object with a characteristic dimension, such as a tree or house, the elevations in the photograph cannot be determined. These objects placed in photographs and maps break down the scale invariance concept, in which case the geological phenomenon does not multiply itself. In geometry, dimension is a property of space, and in common experience the world is three-dimensional: Three measures - length, breath and depth are needed to define volume. In mathematics and physics the concept of dimension is used more abstractly; spaces of four, or even an infinite number of dimensions are

commonly used. Suppose one draws a curved line on paper and then tries to determine its length using either strings or small rulers. One will not be able to come up with a fixed length. A natural assumption would be that as we look at the line more carefully, as we measure it with more detail (smaller rulers), with better vision, the lengths obtained continues to converge to the true value. This is therefore a line with two well defined end points, but without a length. Then what dimension is it? It has a fractional dimension somewhere in between a line and a surface, between 1 and 2 dimensional. So actually, an infinite number of dimensions can be conceptualized in our three dimensional world, never minding the 4<sup>th</sup>, 5<sup>th</sup> and 6<sup>th</sup> dimensions. Fractal dimension, in a rough sense, measures how complicated an object is. It quantifies the "static geometry" of the object. Fractal dimension is defined formally as the limit of the quotient of the log change in object size and the log change in measurement scale, as the measurement scale approaches zero. That is in the limit as  $r \rightarrow 0$ ,

$$D = \frac{\log N}{\log r} \quad (1)$$

where,  $D$  = fractal dimension

$N$  = object size

$r$  = measurement scale

Fractals have shown to be more useful in describing natural objects than are Euclidean objects (Mandelbrot, 1982). Commonly cited examples of fractals in nature include coastlines, topographies, river branching patterns, inter-stellar dust, clouds, and many more. However it is important to know that no natural feature is fundamentally fractal. At some point, clearly at the molecular level, the scale invariance breaks down and gives way to another world with its own characteristics and unique scale. So the scale invariance only exist for a range of scales, from a scale which includes the entire feature being analyzed, down to a small enough scale where we enter new physical worlds. However, the important thing to remember is that fractal models can successfully describe natural features over many orders of magnitude. Consider a mountain ridge some 1 km long made primarily of a sand stone. By the time we get down to the grain size of several millimeters, we would leave the scale invariant behaviour controlled by fracture planes, and individual sand grains will control the profile shape. The grains outlines themselves may have different fractal relationships. So a fractal relationship might exist from 1 km to mms, or over 5 to 6 orders of magnitude. As with most

mathematical descriptions of our world it only works for part of that world. However it has been shown that the restricted range of scales of self-similarity is a very important aspect of the fractal characteristics of natural systems (King, 1983; Tatiana *et al.*, 2000; Sunmonu and Dimri, 2001; Mumtaz and Naci, 2002; Bansal and Dimri, 2005). Most fractals are analyzed using spectral techniques because scaling law such as the power law dependence are preserved by Fourier transforms (Voss, 1988). For example, topography can be analyzed along a linear scale by determining the coefficients  $A_n$  in a Fourier series as a function of wavelengths  $C_n$ , and subsequently determine if the amplitudes  $A_n$  have a power law dependence on the wavelengths. Power law spectra are defined by two quantities, namely the amplitude and the slope, which are used for the purpose of fractal analysis: the slope is a measure of the scaling behaviour of the distribution. In the case of topography Turcotte (1992) showed that the amplitudes are a measure of roughness. Turcotte (1992) also showed that the relationship between the spectral slope  $\tilde{\alpha}$  (known as scaling exponent) and the fractal dimension  $D$  is

$$\lambda = 5 - 2D \quad (\text{for a one-dimensional distribution})$$

$$\lambda = 7 - 2D \quad (\text{for a two-dimensional distribution})$$

Just as a geophysical parameter (e.g. magnetic susceptibility or density) may look similar for a wide range of scale of data, the field generated by this source can also exhibit fractal behaviour. Maus and Dimri (1994) gave the relationship between the scaling exponent of the source and field (for a magnetic distribution) as

$$\gamma = \beta + 1 \quad (2)$$

where,

$\gamma$  = scaling exponent source (susceptibility)

$\gamma$  = scaling exponent of field (magnetic field)

### 3.0 Methods

Rather than moving along a profile (Maus and Dimri, 1995), here a three-dimensional data is considered. A single source was first considered, and the field generated by this source is shown in Figure 1a. This source is a three-dimensional vertical prism uniformly magnetized in the direction of the geomagnetic field and assuming an ambient field of 33,000 gamma. The geomagnetic field inclination and declination is 2° and 4° respectively. The data generated by the

field was calculated using the method of Bhattacharyya (1964) on a 160 by 208 regular grid at 10 km interval, and the prism is 50 km wide along the x-direction (assumed parallel to the north-south direction), 50 km wide (y-direction) and 12 km thick (z-direction). Its top is located 4 km below the plain of measurement and the magnetic susceptibility is 0.011 S.I. unit. Using a data window of 32 km by 32 km, the power spectrum was computed by first finding the Fourier transform of the data and then averaging the square of the Fourier coefficients over constant frequency

intervals. The result was then plotted on a log-log graph, and a line of best-fit was used to obtain a value of  $\beta$  which is the scaling exponent of the field. This was done continuously each time moving the data window until the entire area was covered. The values of  $\beta$  computed at each window were plotted and contoured and the result is shown in figure 1b. Different kinds of shading have been used so as to differentiate susceptibility contrasts. It can be seen in Figure 1b that the source was successfully mapped with the contour line approximating the boundary of the source.

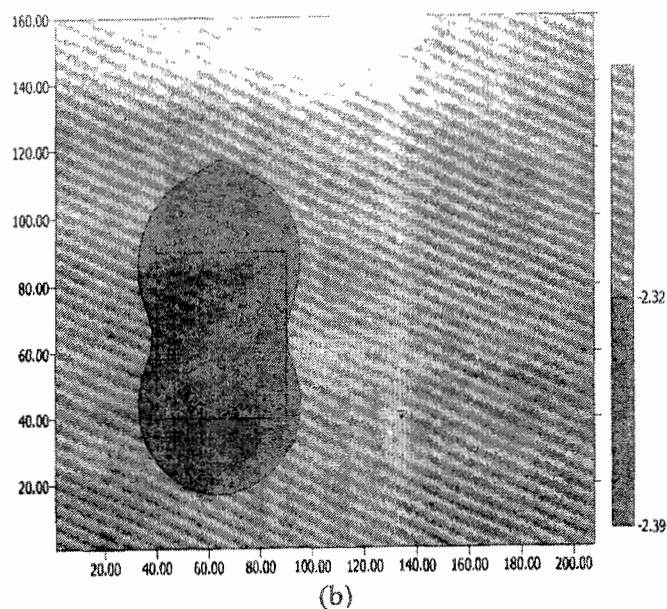
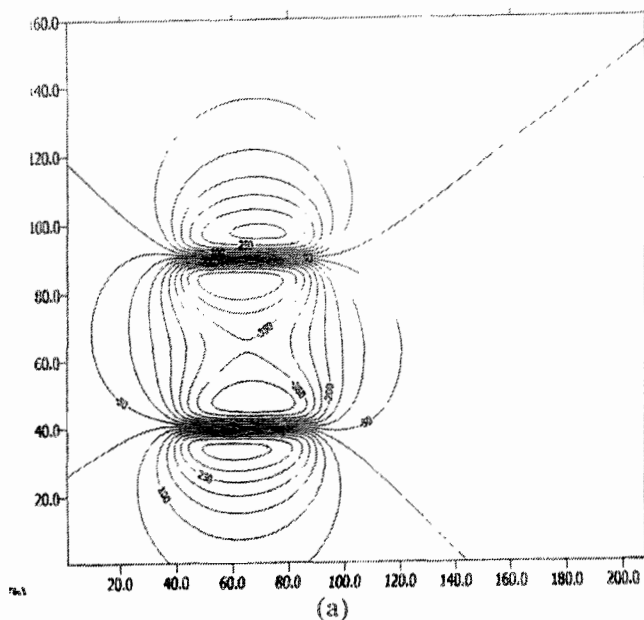


Fig. 1: (a) A three-dimensional vertical prism uniformly magnetized in the direction of the geomagnetic field and assuming an ambient field of 33,000 gamma. Contour interval is 50 nT. (b) Contour map showing variation of scaling exponent of the results obtained from (a).

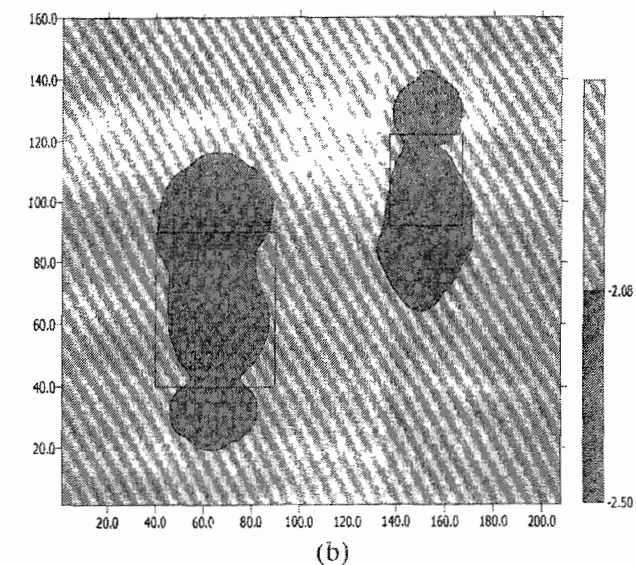
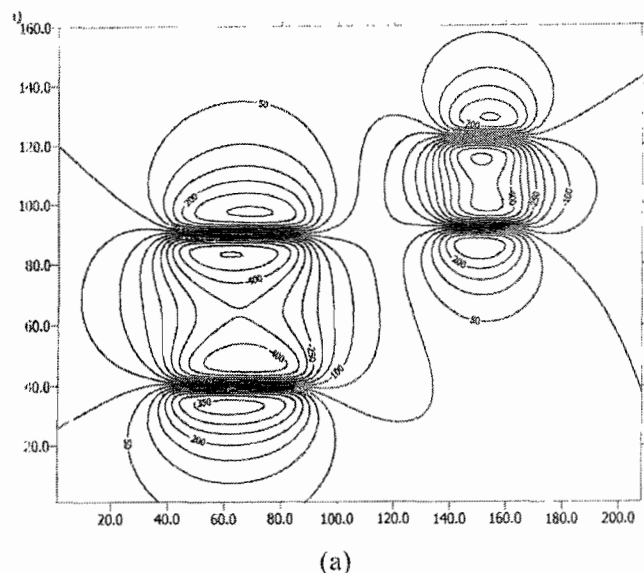


Fig. 2: (a) Field generated by two sources. Contour interval is 50 nT. (b) Contour map showing variation of scaling exponents of the results obtained from the two sources in (a)

To investigate the situation where there are multiple sources, which is often the case in practice, another source was placed close to the source in Figure 1a, and the field generated by both sources is shown in Figure 2a. The new source has a dimension of 30 km by 30 km along the x and y-directions respectively, and is of the same thickness and susceptibility contrast as the first source. The above technique was then applied using the data in figure 2a and the result is shown in figure 2b. It can be seen in figure 2b that the method has clearly resolved the two sources.

In order to further simulate a real geological situation, a more complex model was designed. Figure 3 shows the plan view of this model and Table1 shows the parameters of the sources. This model consist of two geological provinces with the source B6 (see figure 3) representing an intrusion within the province at the left hand side of the map and figure 4a shows the field generated by this model. The above technique was then applied to the model and the result is shown in figure 4b. It can be observed from figure 4b that the method clearly distinguished the two geological provinces with the contour line approximating the boundary separating the two provinces. Also the intrusion (source B6) at the top left hand corner of the map

was detected. In general these results show that this technique can serve as a powerful tool for defining geology in areas of unknown geology, especially over sedimentary basins covered with sand dunes.

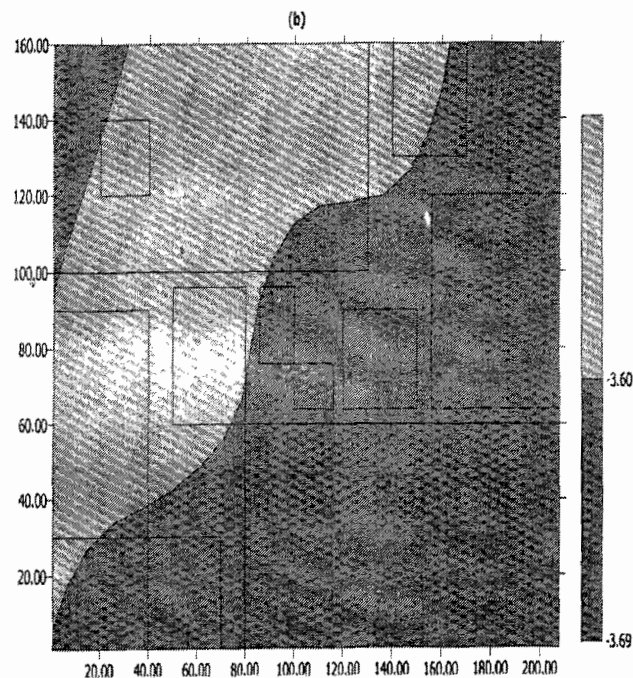
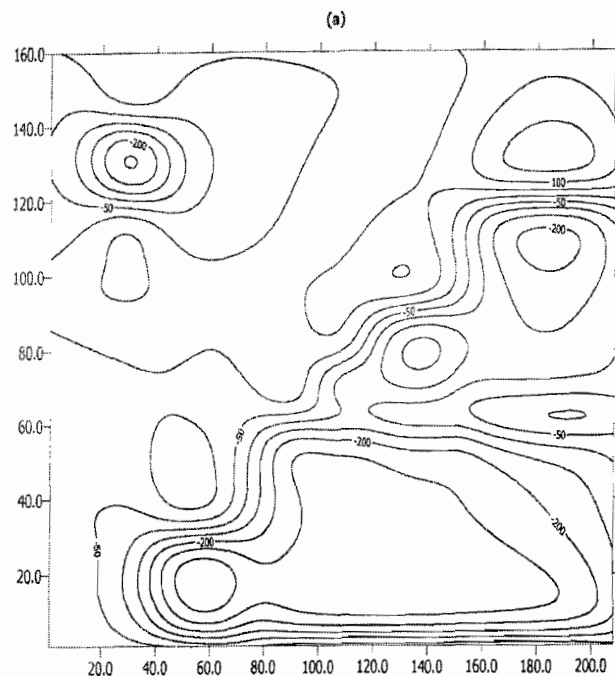


Fig. 4: (a) Field generated by the model in Figure 3. Contour interval is 50 nT. (b) Contour map showing variation of scaling exponents of the results obtained from (a).

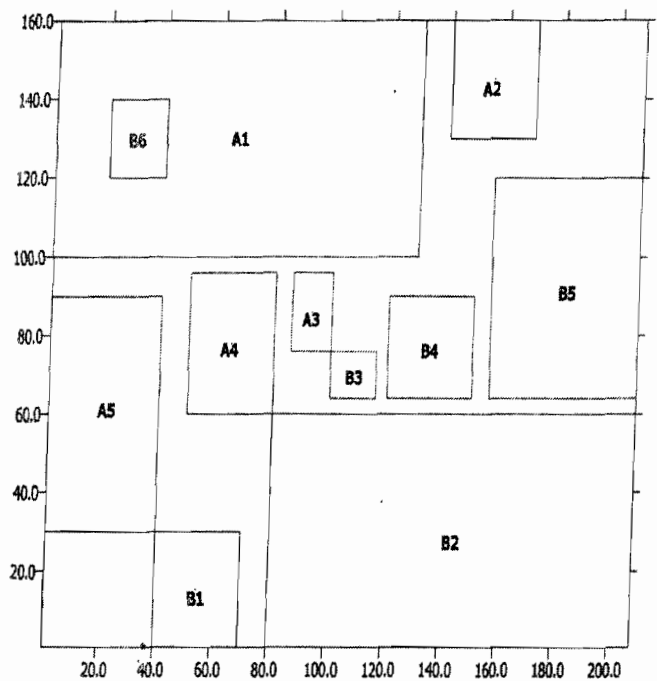


Fig. 3: Plan view of model representing two geological provinces. The source B6 represents an intrusion into one of the province.

4.0 Test on Real Data

The technique described above was applied to three different areas of known geology both for basement complex and sedimentary basin to study how the scaling exponents vary with different geological environments. The data used in these areas were continued down to surface level so that the scaling exponents were determined at the source level. The results of the study are described below.

4.1 The Mamfe Basin

The Mamfe Basin is a sedimentary basin located on both sides of the Nigeria/Cameroon border and is bounded by latitudes 5°30'N to 6°00'N and longitudes 8°15'E to 9°45'E (Figure 5). The basin, and the adjacent Benue Trough, have received considerable attention of many researchers and was selected as one of the test study areas here because it represents a region of contrasting geological

terrain whose magnetic data, which is readily available, was the subject of a recent detailed study by Kangkolo (1995), Ojo and Kangkolo (1997), and Kangkolo *et al.* (1997). The area thus presents ideal test data with prospects for suitable variation in scaling exponent useful for correlation with geology. The Mamfe basin comprises the Precambrian basement, Cretaceous sedimentary rocks (mainly of Albian and Cenomanian age) and intrusive/extrusive rocks associated with Tertiary to recent volcanic episodes. Figure 6 shows the total magnetic field residual anomaly and figure 7a shows the geology of the Mamfe basin which comprises the Precambrian basement, Cretaceous sedimentary rocks (mainly of Albian and Cenomanian age) and intrusive/extrusive rocks associated with Tertiary to recent volcanic episodes.

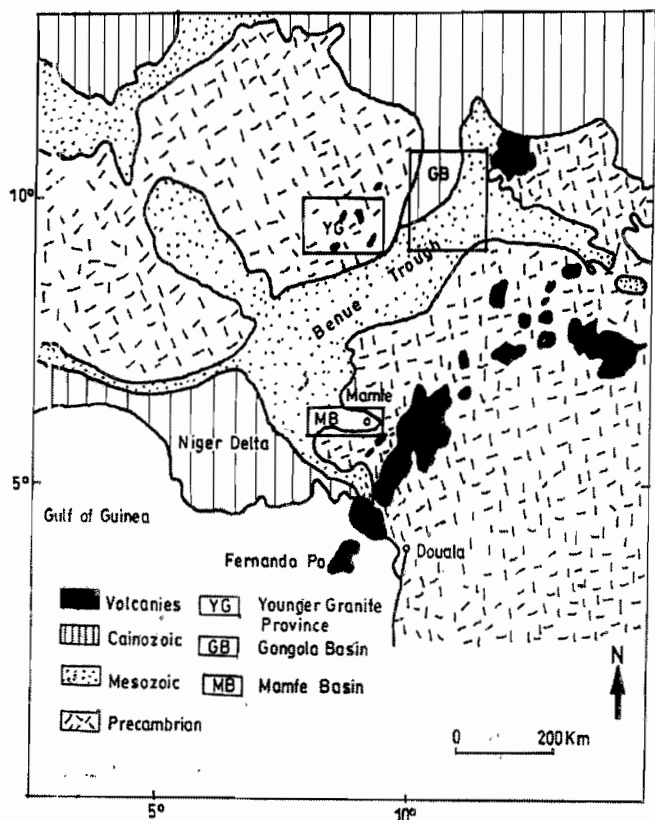


Fig. 5: Map showing the three different areas (the Mamfe basin, the Gongola basin and the Younger Granite province) in which the fractal technique was tested.

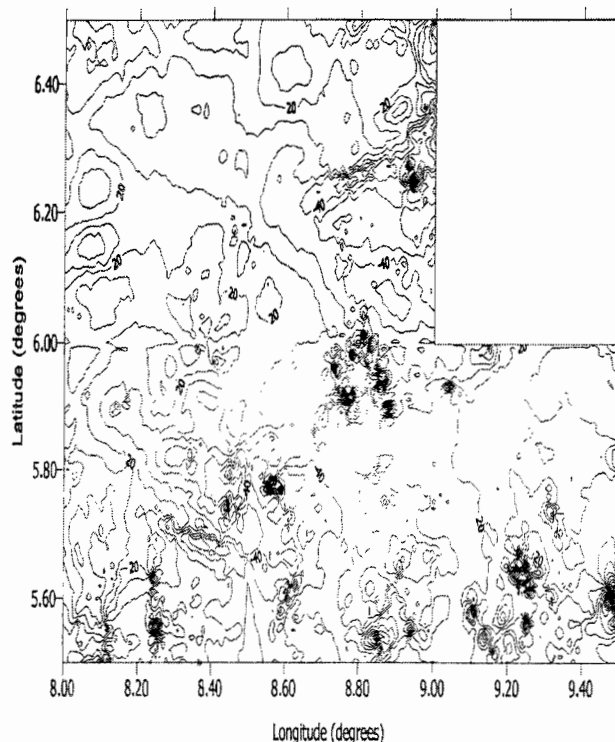


Fig. 6: Map showing the total magnetic field residual anomaly of the Mamfe basin. Contour interval is 20 nT.

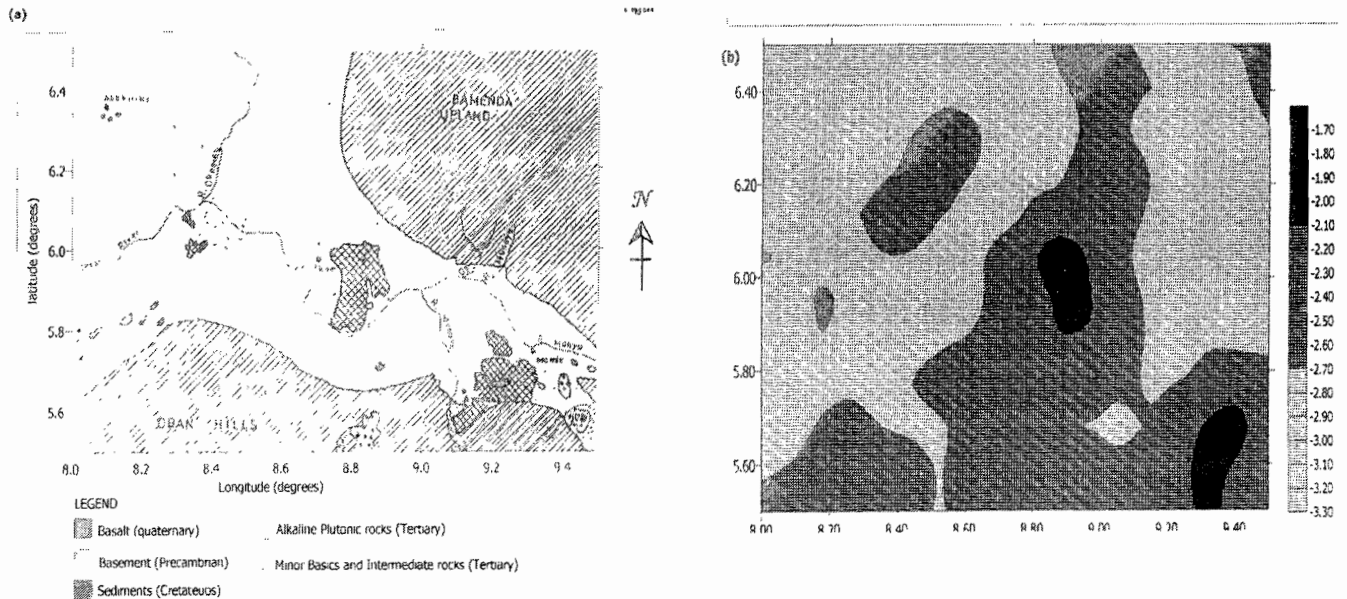


Fig. 7: (a) Geological map of the Mamfe basin (After Kangkolo, 1995)  
 (b) Contoured map of the Mamfe basin showing the variation of scaling exponents.

The procedure described in section 3.0 above was applied to the magnetic data shown in figure 6 and the results show that the scaling exponents vary from -3.30 to -1.70. These values were then contoured and divided into three broad ranges represented by the following shadings: black (-2.10 to -1.70), cross hatched (-2.70 to -2.20), dotted (-3.30 to -2.80) and the result is shown in figure 7b. The figure shows that the scaling exponents are characterized by a dominant NE-SW trend which, while not correlating with the NE-SW trend of the basin geometry and the E-W trend of the regional magnetic anomaly (Kangkolo, 1995), nevertheless is in good agreement with the major trend of the structures of the adjacent Benue Trough to the West and the Cameroon Volcanic Line to the East of the Mamfe basin. Secondly, a comparison of the fractal map (figure 7b) with the geological map (figure 7a) shows that the basalts appear to correspond to the regions mapped with the black shading in the fractal map. In addition, the dotted areas of the fractal map appear to represent the deep portions of the basin while the cross hatched areas represent uplifted or shallow basement which leads to the conclusion that the sedimentary thickness around the central part of the basin is very thin. It may thus be tentatively concluded that in sedimentary terrains, low numerical values of scaling exponents represent shallow basement regions, while high numerical values corresponds to deep sedimentary regions.

#### 4.2 The Gongola basin

The Gongola basin is located at the north-eastern end of the Upper Benue Trough (Figure 5) where the trough bifurcates into an E-W trending Yola arm and a N-S trending Gongola arm otherwise known as the Gongola basin. The aeromagnetic data used in this study covers an area which extends from latitudes 9°30'N to 11°00'N and longitudes 10°00'E to 11°30'E (Abubakar, 2004) as shown in Figure 8. The geological map (Figure 9a) shows that the area comprises the crystalline basement consisting of scattered remnants of highly metamorphosed sedimentary rocks, diverse predominantly granitic plutonic masses of the Older Granite suite and some granite relics of metasedimentary rocks which are found only as xenoliths and small pendants in the granitic rocks (Cater et al., 1963). A sedimentary sequence made up of the Bima Sandstones, Gombe Formation, Pindiga Formation, and the Yolde Formation with a prominent NE-SW trend dominates the area while basement rocks also outcrop as an inlier around Kaltungo. Application of the procedure in section 3.0 produces a fractal map shown in figure 9b, and a comparison of this with the geologic map of the area (Figure 9b) indicates very good correlations between the two maps. An interesting

observation from this result is that the NE-SW strike of the geological map has been perfectly reproduced in the fractal map. The scaling exponents in the fractal map (Figure 9b) vary from -3.20 to -2.20 and the contoured values have been divided into two ranges: cross-hatched shading representing scaling exponent values from -2.60 to -2.20, and dotted shading representing scaling exponent values from -3.20 to -2.61. It is also observed here, just as is in the Mamfe basin, that low numerical values of scaling exponents represent shallow basement regions, while high numerical values correspond to deep sedimentary regions. The cross-hatched shaded region in the south-eastern part of the fractal map is in good correlation with the occurrence of the Kaltungo inlier. Therefore, the other diagonally shaded region occurring in the north-eastern part of the fractal map suggests that the basement rock around that region might be highly elevated. This is consistent with the interpretations by Abubakar (2004) from spectral analysis of the magnetic data.

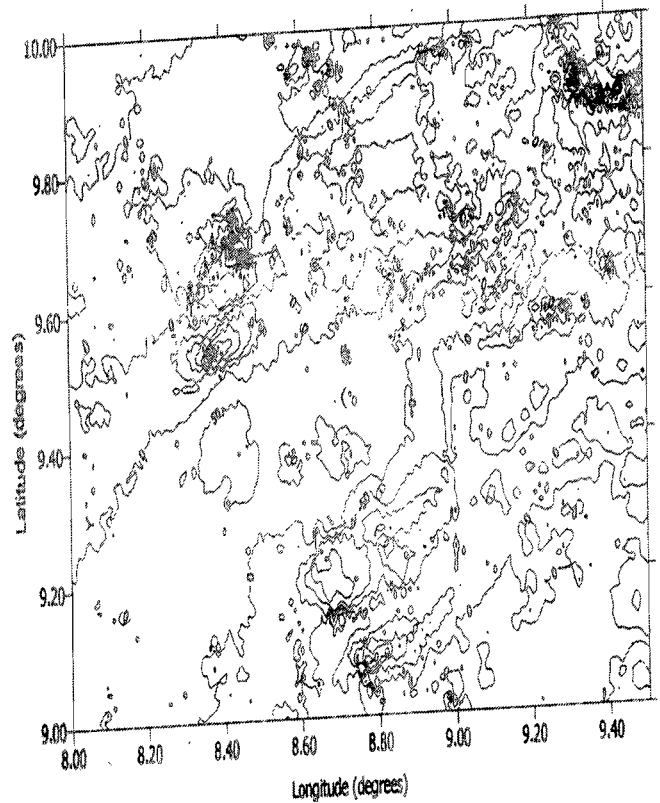


Fig. 8: Map showing the total magnetic field residual anomaly of the Gongola basin. Contour interval is 50 nT.

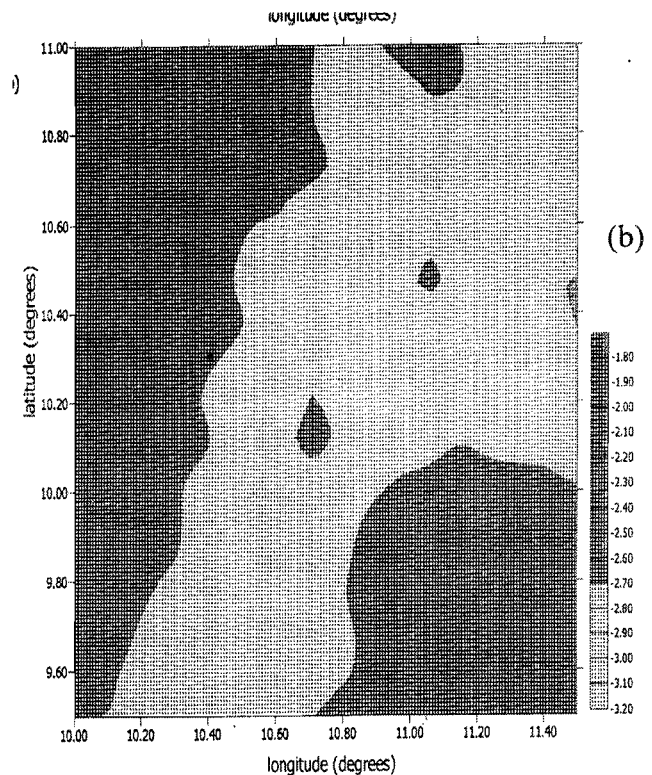
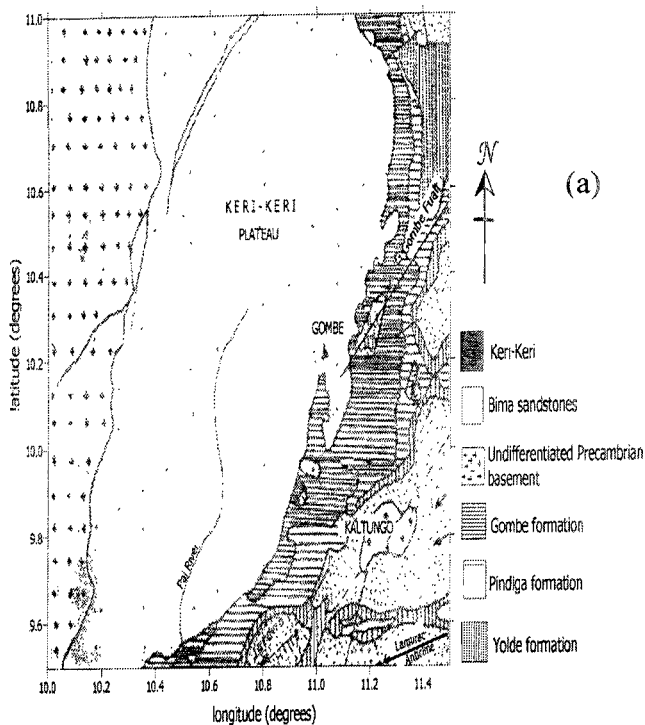


Fig. 9: (a) Geological map of the Gongola basin (After Abubakar, 2004).  
 (b) Contoured map of the Gongola basin showing the variation of scaling exponents.

### 4.3 The Younger Granite province

The Younger Granite province forms part of the central Plateau of Nigeria and comprises of the Precambrian to Lower Paleozoic Basement Complex into which the Jurassic Younger Granite Complex are intruded (Figure 5). Figure 10 shows the total magnetic field residual anomaly for the area of study and the interpretations done on this area by Pascal (2001) indicated an east-west trend for the regional field within the area. The data used in this area covers an area extending from latitudes 9°00' to 10°00' North and longitudes 8°00' to 9°30' East. Many geological/geophysical works have been done in the Younger Granite Province. Ajakaiye *et al.* (1985) interpreted aeromagnetic data over the area and found NE-SW trending anomalies as the dominant magnetic features, possibly representing tectonic trends through which the Younger Granite complexes were intruded. On a more detailed scale, structures in the basement appeared to have influenced the location of each ring complex (Turner,1973). Therefore, alignments of the ring complexes follow a number of different directions with no single dominant trend. Figure 11a shows the geology of the area. The Younger Granite ring complexes are circular or elliptical intrusions and the general sequence in their emplacement has been described by Macleod *et al.* (1971). The technique in section 3.0 was applied to the data in figure 10 and the result is shown in figure 11b. The scaling exponents for figure 11b have values which vary from -3.40 to -2.30, and these have been divided into four groups represented by the following shadings: white (-

2.60 to -2.30) cross-hatched (-2.80 to -2.61), dotted (-3.00 to -2.81) and black (-3.40 to -3.01). It can be seen in figure 11b that the black areas have good correlation with the Younger granite rocks on the geological map of the area, while the dotted area corresponds well with the basalt flows. The cross-hatched shaded area on the fractal map represents the undifferentiated basement in which the Older Granites, represented as white have intruded. Therefore the white region which occurs at the south western part of the fractal map is most likely to be an unexposed Older Granite intrusion. A general overview of the fractal map (Figure 11b) indicates that most of the structures within the area have an E-W trend, which corresponds to the E-W regional field obtained by Pascal (2001).

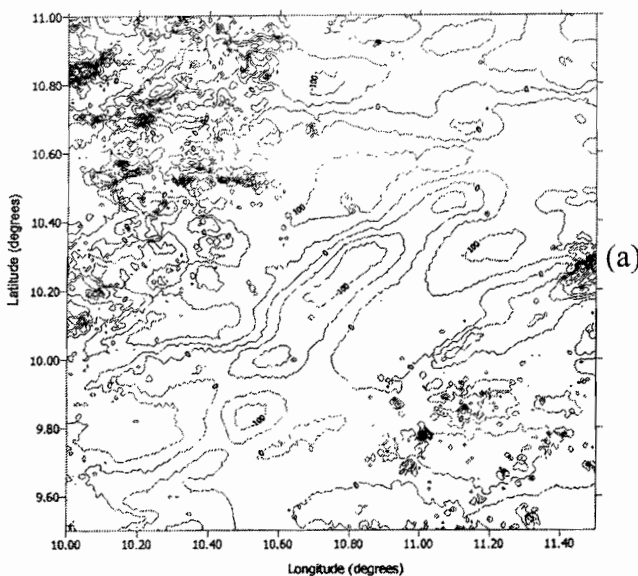


Fig. 10: Map showing the total magnetic field residual Anomaly of the Younger Granite province. Contour interval is 50 nT.

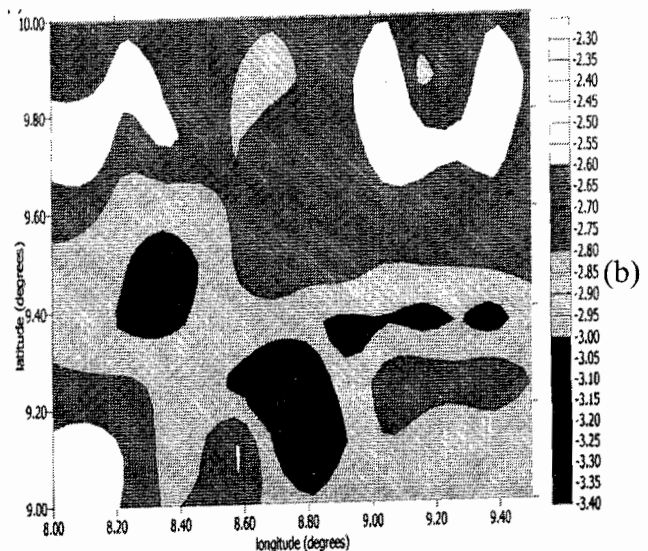
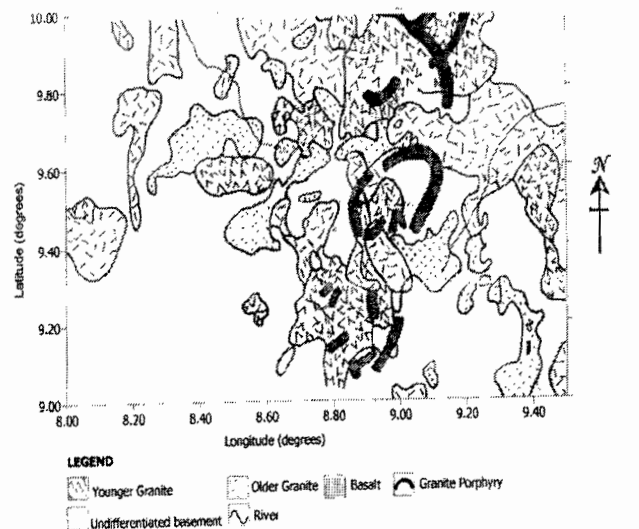


Fig. 11: (a) Geological map of the Younger Granite province (After Pascal, 2001). (b) Contoured map of the Younger Granite province showing the variation of scaling exponents.



Table 1: Parameters of the sources in Figure 3.

BODY	LENGTH $a_1$ (km)	LENGTH $a_2$ (km)	WIDTH $b_1$ (km)	WIDTH $b_2$ (km)	DEPTH TO TOP $h_1$ (km)	DEPTH TO BOTTOM $h_2$ (km)	SUSCEP TIBILITY (S.I. Unit)
A1	100	160	1	130	5	20	0.001
A2	130	160	140	170	5	20	0.001
A3	76	96	86	100	5	20	0.001
A4	60	96	50	80	5	20	0.001
A5	30	90	1	40	5	20	0.001
B1	1	30	40	70	5	20	0.011
B2	1	60	80	208	5	20	0.011
B3	64	76	100	116	5	20	0.011
B4	64	90	120	150	5	20	0.011
B5	64	120	156	208	5	20	0.011
B6	120	140	20	40	5	20	0.011

### 5.0 Conclusion

The use of scaling exponent for geophysical mapping has been investigated using both theoretical and real data. Results from the analysis with theoretical data showed that the scaling exponent was able to map isolated sources, but could not properly resolve bodies that were close to each other. Application to real data was done on three different areas of known geology. These areas are the Mamfe basin, the Gongola basin and the Younger Granite province, and the results obtained showed good correlation between the geological map and the fractal map for each area. A close observation of the fractal maps of the Mamfe Basin and the Gongola basin shows that the undifferentiated basement rocks have scaling exponent values which vary from -2.68 to -2.37 in the Mamfe basin and -2.60 to -2.20 in the Gongola basin. Also the fractal map for the Younger Granite complex show that the undifferentiated basement rock within the area has scaling exponent ranging from -2.8 to -2.6. It can therefore be assumed that the scaling exponents representing basement rock generally have values between -3.0 and -2.0. This technique can therefore be applied to areas of unknown geology or mapping of the basement geology of sedimentary basins. The above results have also shown that the fractal map serve as a very good aid in geological interpretation as an alternative to the use of the total magnetic field map only.

### References

- Abubakar, Y.I., (2004): An Investigation of a Prominent Aeromagnetic Anomaly Within the Gongola Basin (Upper Benue Trough), M.Sc. thesis (unpublished), Ahmadu Bello University, Zaria, Nigeria.
- Ajakaiye, D.E., Hall D.H. and Miller, T.W., (1985): Interpretation of Aeromagnetic Data Across the Central Crystalline Shield of Nigeria. *Geophysical Journal of the Royal Astronomical Society of Nigeria*, 83, 503-517.
- Bansal A.R. and Dimri V.P., (2005): Depth Determination From a Non-stationary Magnetic Profile for Scaling Geology. *Geophysical Prospecting*, 53, 399-410.
- Bhattacharyya, B.K., (1964): Magnetic Anomalies Due to Prism-shaped Bodies With Arbitrary Polarization, *Geophysics*, 29, 517-531.
- Carter, J. D., Barber W. and Jones, G.P., (1963). The Geology of parts of Adamawa, Bauchi and Bornu Provinces in northeastern Nigeria, *Geological Survey of Nigeria Bulletin*, 30, 99pp.
- Kangkolo, R., (1995): A Detailed Interpretation of the Aeromagnetic Field Over the Mamfe

- Basin of Nigeria and Cameroon. Ph.D Thesis (unpublished), Physics Department, Ahmadu Bello University-Zaria.
- Kangkolo, R., Ojo, S.B. and Umego, M.N., 1997. Estimation of Basement Depths in the Middle Cross River Basin by Spectral Analysis of Aeromagnetic Fields. *Nigerian Journal of Physics*, 9, 30-36.
- King, G. (1983): The Accommodation of large strains in the Upper Lithosphere of the Earth and Other Solids by Self-similar Fault Systems: The Geometrical Origin of B-value. *Pure and Applied Geophysics*, 121, 761-815.
- Macleod, W.N., Turner, D.C. and Wright, E.P. (1971): The Geology of Jos Plateau: General Geology. *Bulletin of the Geological Survey of Nigeria*, 32, 112pp.
- Mandelbrot, B. B., (1982): *The Fractal Geometry of Nature*, Freeman, San Francisco, 216pp.
- Maus, S. and Dimri, V.P., (1994) Scaling Properties of Potential Fields Due to Scaling Sources. *Geophysical Research Letters*, 21, 891-894.
- Maus, S. and Dimri V., (1995): Potential Field Power Spectrum Inversion for Scaling Geology. *Journal of Geophysical Research*, 100, (B7), 12605-12616.
- Mumtaz, H. and Naci O., (2002): Determination of Crustal Density at the Atmosphere-crust Interface of Western Anatolia by Using the Fractal Method. *Journal of the Balkan Geophysical Society*, 5, 3-8.
- Ojo, S.B. and Kangkolo, R., (1997). Short Comings in the Determination of Regional Fields by Polynomial Fitting: A simple Solution. *Journal of Applied Geophysics*, 36, 205-212.
- Pascal, A.F., (2001): Interpretation of the Aeromagnetic Anomalies over the South-western part of the Younger Granite Province in North-central Nigeria, M.Sc. Thesis (unpublished), Ahmadu Bello University, Zaria, Nigeria.
- Pilkington, M. and Todoeschuck, J.P., 1993. Fractal Magnetization of Continental Crust. *Geophys. Res. Lett.*, 20, 627-630.
- Sunmonu L.A. and Dimri V.P., 2001. Multifractal Analysis and Siesmicity of the Himalayan Region-A Case Study. *Nigerian Journal of Physics*, 13, 106-111.
- Tatiana Q., Fedi M. and De Santis A., (2000): Source Ambiguity from an Estimation of the Scaling Exponent of Potential Field Power Spectra, *Geophysical Journal International*, 140, 311-323.
- Turcotte, D.L., (1992): *Fractals and Chaos in Geology and Geophysics*; Cambridge Univ. Press, 221pp.
- Turner, D.C., (1973): Structure and Tectonic Setting of the Younger Granite Ring Complexes of Nigeria and Southern Niger, Part I: Ring Complexes and their Component Units. *Savanna*, 1, 223-236.
- Voss, R. F., (1988): *Fractals in Nature: From Characterization to Simulation*, in *The Science of Fractal Images*, H. O. Peitgen and D. Saupe, eds, 21-70, Springer-Verlag, New York.